

Article

Facile One-Pot Multicomponent Synthesis of Pyrazolo-Thiazole Substituted Pyridines with Potential Anti-Proliferative Activity: Synthesis, In Vitro and In Silico Studies

Islam H. El Azab ^{1,*} , Rania B. Bakr ²  and Nadia A. A. Elkanzi ^{3,4}

¹ Food Science and Nutrition Department, College of Science, Taif University, P.O. Box 11099, Taif 21944, Saudi Arabia

² Department of Pharmaceutical Organic Chemistry, Faculty of Pharmacy, Beni-Suef University, Beni-Suef 62514, Egypt; rbbakr@ju.edu.sa

³ Chemistry Department, College of Science, Jouf University, P.O. Box 2014, Sakaka, Saudi Arabia; nahasan@ju.edu.sa

⁴ Chemistry Department, Faculty of Science, Aswan University, Aswan, P.O. Box 81528, Aswan, Egypt

* Correspondence: i.helmy@tu.edu.sa

Abstract: Pyrazolothiazole-substituted pyridine conjugates are an important class of heterocyclic compounds with an extensive variety of potential applications in the medicinal and pharmacological arenas. Therefore, herein, we describe an efficient and facile approach for the synthesis of novel pyrazolo-thiazolo-pyridine conjugate **4**, via multicomponent condensation. The latter compound was utilized as a base for the synthesis of two series of 15 novel pyrazolothiazole-based pyridine conjugates (**5–16**). The newly synthesized compounds were fully characterized using several spectroscopic methods (IR, NMR and MS) and elemental analyses. The anti-proliferative impact of the new synthesized compounds **5–13** and **16** was in vitro appraised towards three human cancer cell lines: human cervix (HeLa), human lung (NCI-H460) and human prostate (PC-3). Our outcomes regarding the anti-proliferative activities disclosed that all the tested compounds exhibited cytotoxic potential towards all the tested cell lines with $IC_{50} = 17.50–61.05 \mu M$, especially the naphthyridine derivative **7**, which exhibited the most cytotoxic potential towards the tested cell lines ($IC_{50} = 14.62–17.50 \mu M$) compared with the etoposide ($IC_{50} = 13.34–17.15 \mu M$). Moreover, an in silico docking simulation study was performed on the newly prepared compounds within topoisomerase II (3QX3), to suggest the binding mode of these compounds as anticancer candidates. The in silico docking results indicate that compound **7** was a promising lead anticancer compound which possesses high binding affinity toward topoisomerase II (3QX3) protein.

Keywords: *N*-Heterocycles; multicomponent condensation; pyrazole-3-carbothioamide; thiazole; pyran; pyridine; anticancer activity; molecular docking



Citation: El Azab, I.H.; Bakr, R.B.; Elkanzi, N.A.A. Facile One-Pot Multicomponent Synthesis of Pyrazolo-Thiazole Substituted Pyridines with Potential Anti-Proliferative Activity: Synthesis, In Vitro and In Silico Studies. *Molecules* **2021**, *26*, 3103. <https://doi.org/10.3390/molecules26113103>

Academic Editors: David Díez, María Ángeles Castro and Bartolo Gabriele

Received: 15 April 2021

Accepted: 19 May 2021

Published: 22 May 2021

Publisher's Note: MDPI stays neutral with regard to jurisdictional claims in published maps and institutional affiliations.



Copyright: © 2021 by the authors. Licensee MDPI, Basel, Switzerland. This article is an open access article distributed under the terms and conditions of the Creative Commons Attribution (CC BY) license (<https://creativecommons.org/licenses/by/4.0/>).

1. Introduction

The majority of the developed anticancer chemotherapies are not very effective, and side effects might concurrently occur, such as drug-induced impedance. Thus, there is still a critical need to develop novel effective and safe medicines with fewer side effects for the durable treatment of cancer [1,2]. Nitrogen-containing heterocyclic motifs are of high interest owing to their applications as pharmacologically active molecules. These molecules have gained cumulative attention, so they have contributed to the improvement of plentiful organic synthesis protocols and found ample applications in the chemical sciences [3–7]. Several *N*-heterocyclic conjugates are widely dispersed in nature and are constituents of many biologically important molecules, including several vitamins [8], antibiotics [9], nucleic acids [10], dyes and pharmaceuticals [11,12]. Moreover, the characteristics and utilization of *N*-heterocyclic skeletons (Figure 1) have gained a reputation in the rapidly

growing fields of organic and therapeutic chemistry as well as the pharmaceutical industry [13–15]. On the other hand, the electron-donating heterocycle is not only able to readily receive or provide a proton, but it can also simply create various weak connections. Some of the intermolecular connections—for instance, hydrogen-bonding formation, van der Waals forces, dipole–dipole interactions, hydrophobic effects and π -stacking interactions—of *N*-heterocycles have amplified their significance in the field of therapeutic chemistry and allow them to efficiently adhere to a diversity of enzymes and receptors in drugs due to their improved solubility [16–19].

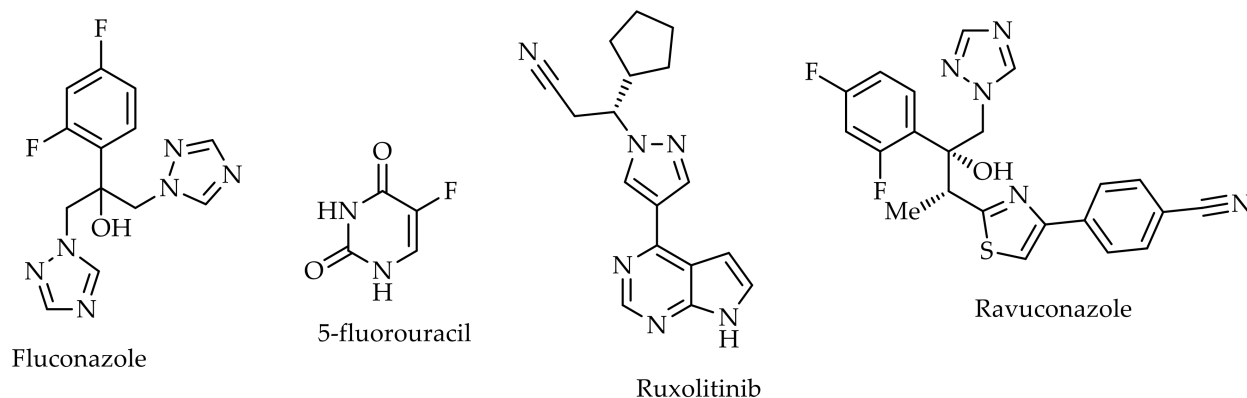


Figure 1. Representative examples of bioactive nitrogen-containing compounds.

Among nitrogen heterocyclic analogues, pyrimidines have numerous applications in medicinal chemistry; the pyrimidine bases of uracil, cytosine and thymine are crucial building blocks of DNA and RNA [20]. In addition, pyrazole-containing scaffolds are a class of heterocycles that exhibit a wide range of biological effects, including anti-cancer [21], anti-HIV [22], antimalarial [23], anti-tubercular [24], anti-microbial [25] and diabetic activities [26,27].

Hybrid molecules containing thiazole scaffolds are a potential set of heterocyclic compounds; a thiazole core has been found in numerous biologically active natural drugs, such as thiamine (vitamin-B1), penicillin and luciferin [28]. There is a vast number of thiazoles that exhibit a wide range of pharmacological activities, including antibacterial [29], anticancer [30], antifungal [31], anti-inflammatory [32], antioxidant [33] and anti-tubercular activities [34]. Therefore, we believe that the merging of pyrazole and thiazole moieties will result in a class of pharmacophores that exhibit promising biological activities; in fact, several previous works have reported their potential activities, such as anticonvulsant, anti-HIV, anti-inflammatory and anticancer activities [35–40].

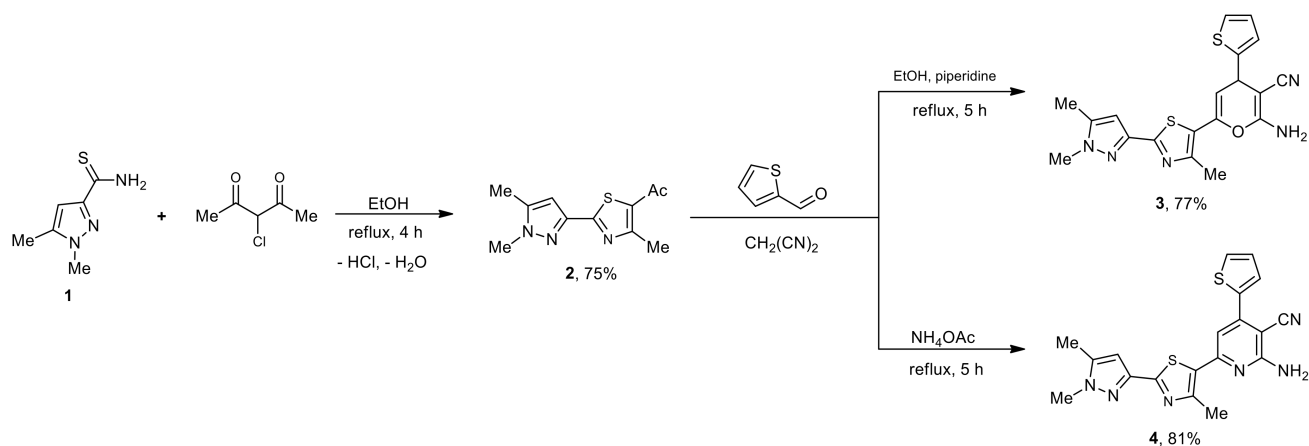
Based on the aforementioned applications of nitrogen-containing heterocycles, as well as the need for the construction of new bioactive *N*-heterocycles [41–47], herein, we report an efficient and facile approach for building up novel nitrogen-containing heterocycles with promising anti-proliferative effects, starting with 2-amino-6-(2-(1,5-dimethyl-1*H*-pyrazol-3-yl)-4-methylthiazol-5-yl)-4-(thiophen-2-yl)nicotinonitrile (4).

2. Results and Discussion

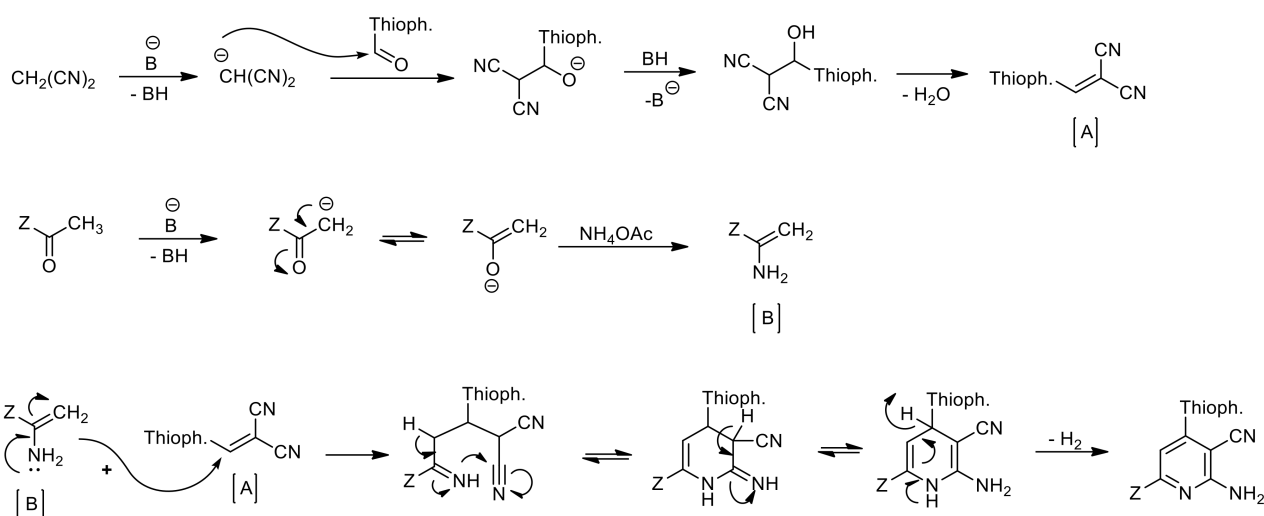
2.1. Chemistry

As an extension of our approach to the intended *N*-heterocycles [41–47], we studied the utilization of 2-(1,5-dimethyl-1*H*-pyrazol-3-yl)-5-acetyl-4-methyl-thiazole (2) to construct a potentially bioactive pyran and/or pyridine hybrids. Thus, coupling of the pyrazolecarbothiamide 1 with 3-chloropentane-2,4-dione in refluxing ethanol afforded the acetyl compound 2 in a 75% yield. Next, a multicomponent reaction of the acetyl compound 2 with thiophene-2-carbaldehyde and malononitrile under reflux in ethanolic piperidine solution yielded the pyran derivative 3. Meanwhile, performing the same reac-

tion with NH_4OAc yielded the pyridine analogue **4** in an 81% yield (Scheme 1). A plausible mechanism for the construction of 2-amino-3-cyano pyridine moiety **4** using NH_4OAc is displayed in Scheme 2, where the intermediate 2-(thiophen-2-ylmethylene)malononitrile [**A**], which was obtained via the coupling of thiophene-2-carbaldehyde and malononitrile, was reacted with the thiazoylenamine [**B**]; subsequently, an intramolecular cyclization, intermolecular rearrangement and auto oxidation yielded the pyridine analogue **4**. The spectral as well as the analytical data of **3** and **4** were consistent with their own structures (see Materials and Methods section).



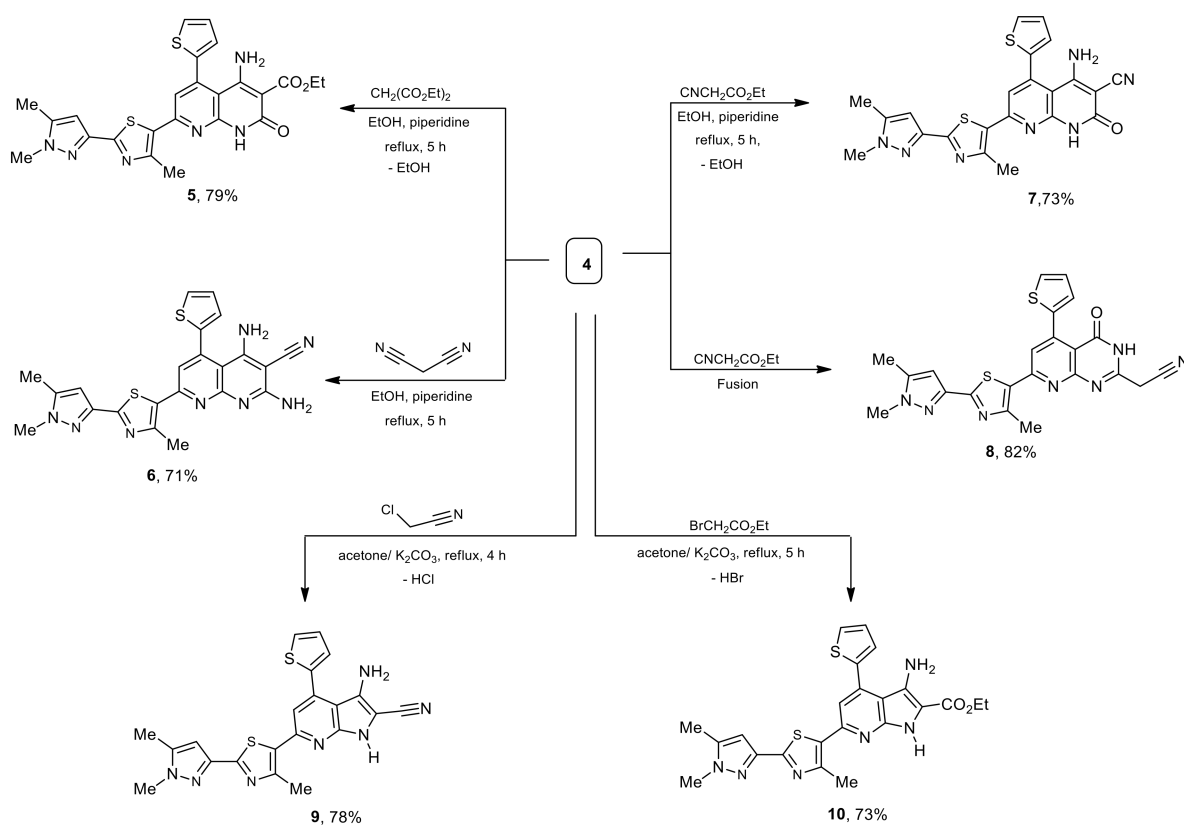
Scheme 1. Synthesis of pyran and pyridine analogues **3** and **4**.



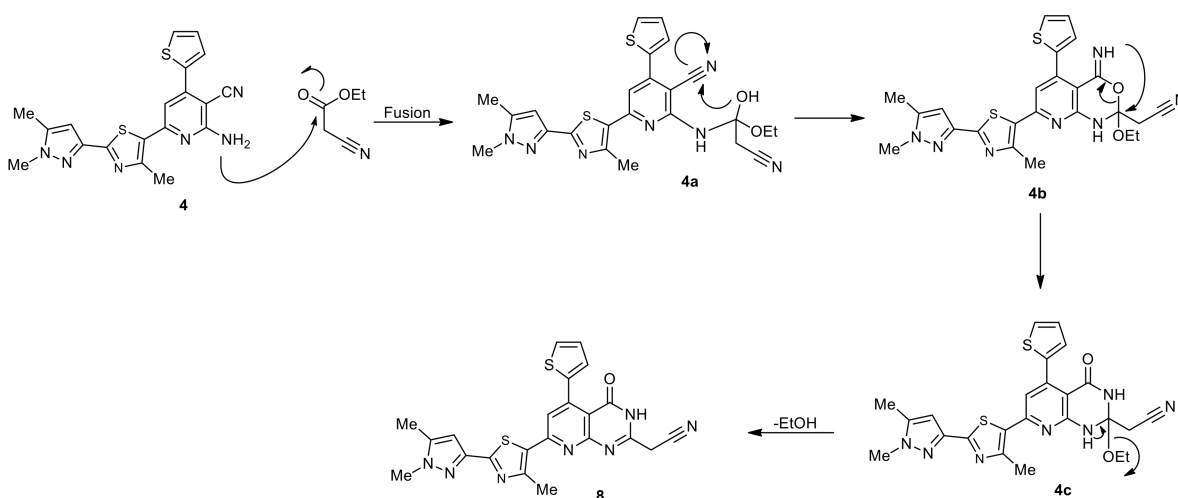
Scheme 2. The plausible mechanism for the formation of 2-amino-3-cyano pyridine core **4**.

Then, the reactivity of the *o*-aminonitrile tag in the pyridine analogue **4** was studied via cyclization with some active methylene compounds, to construct the envisioned pyridine and/or pyrrole nucleus-fused pyridine. Consequently, cyclization of the *o*-aminonitrile pyridine **4** under basic conditions in EtOH with diethylmalonate and malononitrile afforded 4-amino-1,8-naphthyridines (**5** and **6**) in fair yields (Scheme 3). Notably, the reaction product of compound **4** with ethyl cyanoacetate was extremely dependent on the reaction conditions. Thus, compound **4** refluxed with ethyl cyanoacetate in ethanolic piperidine solution yielded the 1,8-naphthyridine derivative **7** in a 73% yield, but when the same reaction was carried out under fusion, it yielded 2-cyanomethylpyrido[2,3-*d*]pyrimidin-4(3*H*)-one analogue (**8**) in an 82% yield. A reasonable mechanism for the formation of compound **8** is presented in Scheme 4. This reaction is assumed to proceed via an inter-

molecular nucleophilic attack of the amino pyridine analogy **4**, on the carbonyl carbon in the ethyl canoacetate, leading to the intermediate **4a**, and subsequent intramolecular cyclization via further, nucleophilic attack by the -OH moiety on the nitrile group afforded the cyanomethylpyrido[2,3-*d*][1,3]oxazine derivative **4b**. The intermediate **4b** undergoing intramolecular Dimroth-like rearrangement afforded the pyrido[2,3-*d*]pyrimidine analogue **4c**, and subsequent elimination of ethanol yielded the pyrido[2,3-*d*]pyrimidine analogue (**8**) (Scheme 4).



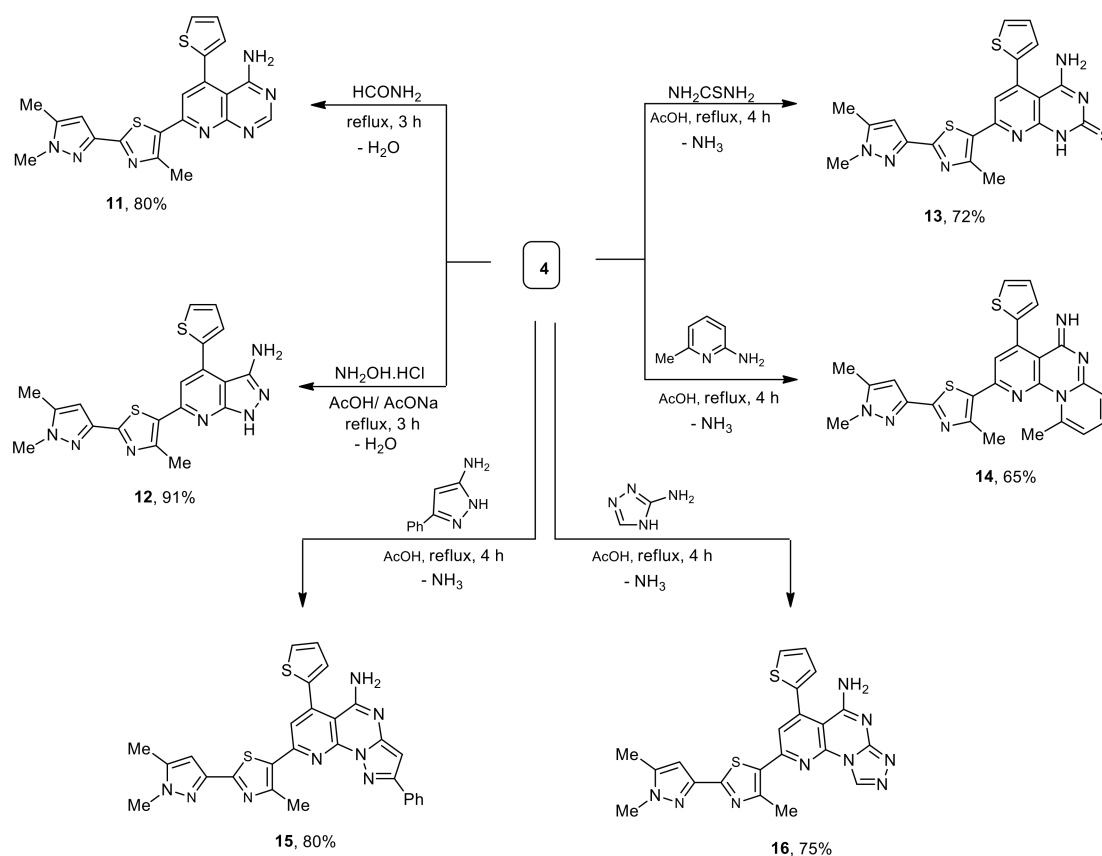
Scheme 3. Synthesis of compounds 5–10.



Scheme 4. The reasonable mechanism for the formation of cyanomethylpyrido[2,3-*d*]pyrimidine derivative (**8**).

Moreover, fusing of a pyrrole nucleus with the pyridine moiety in compound **4** was achieved via the condensation of compound **4** with 2-chloroacetonitrile and/or ethyl bromoacetate in refluxing acetone and anhydrous K_2CO_3 , which led to the new pyrrolo[2,3-*b*]pyridin-3-amine derivatives **9** and **10**, respectively (Scheme 3). The IR spectrum of compound **10** disclosed the lack of nitrile absorption that was initially observed in compound **4** (IR), while new absorption bands at 1664 and 3341 cm^{-1} were assigned to $C=O$ and NH_2 groups separately, and its mass spectrum showed an ion peak at m/z 478.12, which confirmed its molecular formula, $C_{23}H_{22}N_6O_2S_2$. Moreover, the H-resonances of compound **10** showed triplet and quartet signals owing to the ethyl moiety at 1.26 and 4.32 ppm, respectively.

Next, the precursor **4** was subjected to further ring closure by coupling with some amino nucleophiles, which led to a set of pyridopyrimidine analogues (Scheme 5). In consideration of this, we treated compound **4** under reflux with formamide, hydroxylamine hydrochloride, thiourea, 6-methylpyridin-2-amine, 5-amino-3-phenyl-1*H*-pyrazole and/or 3-amino-1,2,4-triazole to construct pyridopyrimidines (**11–16**), in fair yields ranging from 65 to 91% (Scheme 5). The absence of nitrile absorbance was clearly observable in the IR spectra of these compounds. The mass spectrum of compound **16** exposed a molecular ion peak at m/z 459.12, which confirmed its molecular formula ($C_{21}H_{17}N_9S_2$) (see Supplementary Materials).



Scheme 5. Synthesis of compounds **11–16**.

2.2. Evaluation of Biological Impact

2.2.1. Cytotoxic Activity

The newly constructed derivatives **5–13** and **16** were evaluated *in vitro* for their cytotoxic potential towards a prostate cancer cell line (PC-3), lung cancer cell line (NCI-H460) and cervical cancer cell line (Hela) using etoposide as a standard and adapting the MTT assay protocol [48,49]. The obtained outcomes (Table 1, Figure 2) showed that all the

tested compounds exhibited cytotoxic potential against PC-3 ($IC_{50} = 17.50\text{--}65.41 \mu\text{M}$), NCI-H460 ($IC_{50} = 15.42\text{--}61.05 \mu\text{M}$) and Hela ($IC_{50} = 14.62\text{--}59.24 \mu\text{M}$) compared to etoposide ($IC_{50} = 17.15, 14.28$ and $13.34 \mu\text{M}$, respectively). Moreover, 4-Amino-7-(2-(1,5-dimethyl-1H-pyrazol-3-yl)-4-methylthiazol-5-yl)-2-oxo-5-(thiophen-2-yl)-1,2-dihydro-1,8-naphthyridine-3-carbonitrile (**7**) was the most potent candidate towards PC-3 ($IC_{50} = 17.50 \mu\text{M}$), NCI-H460 ($IC_{50} = 15.42 \mu\text{M}$) and Hela ($IC_{50} = 14.62 \mu\text{M}$), which, in addition, revealed comparable anticancer potential to that exhibited by the standard drug etoposide ($IC_{50} = 17.15, 14.28$ and $13.34 \mu\text{M}$, respectively). The pyridotriazolopyrimidin-5-amine analogy **16** was the least active candidate ($IC_{50} = 65.41, 61.05$ and $59.24 \mu\text{M}$, respectively) towards the three tested cell lines, PC-3, NCI-H460 and Hela.

Table 1. In vitro cytotoxic results of the target compounds **5–13**, **16** and etoposide towards PC-3, NCI-H460 and Hela cell lines.

Compound No.	In Vitro Cytotoxicity IC_{50} (μM) \pm SD		
	PC-3	NCI-H460	Hela
5	29.31 \pm 0.91	27.54 \pm 0.43	25.73 \pm 1.62
6	22.73 \pm 1.40	21.12 \pm 1.31	19.31 \pm 0.45
7	17.50 \pm 0.35	15.42 \pm 0.32	14.62 \pm 0.52
8	28.62 \pm 1.15	26.92 \pm 0.32	26.31 \pm 0.46
9	35.12 \pm 0.26	32.81 \pm 0.51	31.05 \pm 0.87
10	48.29 \pm 0.36	47.12 \pm 1.08	45.62 \pm 1.34
11	59.13 \pm 1.12	58.64 \pm 1.41	58.12 \pm 0.41
12	49.08 \pm 0.92	48.13 \pm 0.52	47.13 \pm 0.95
13	56.71 \pm 0.87	55.03 \pm 0.61	53.76 \pm 1.67
16	65.41 \pm 0.75	61.05 \pm 0.75	59.24 \pm 1.20
Etoposide	17.15 \pm 0.24	14.28 \pm 0.15	13.34 \pm 0.23

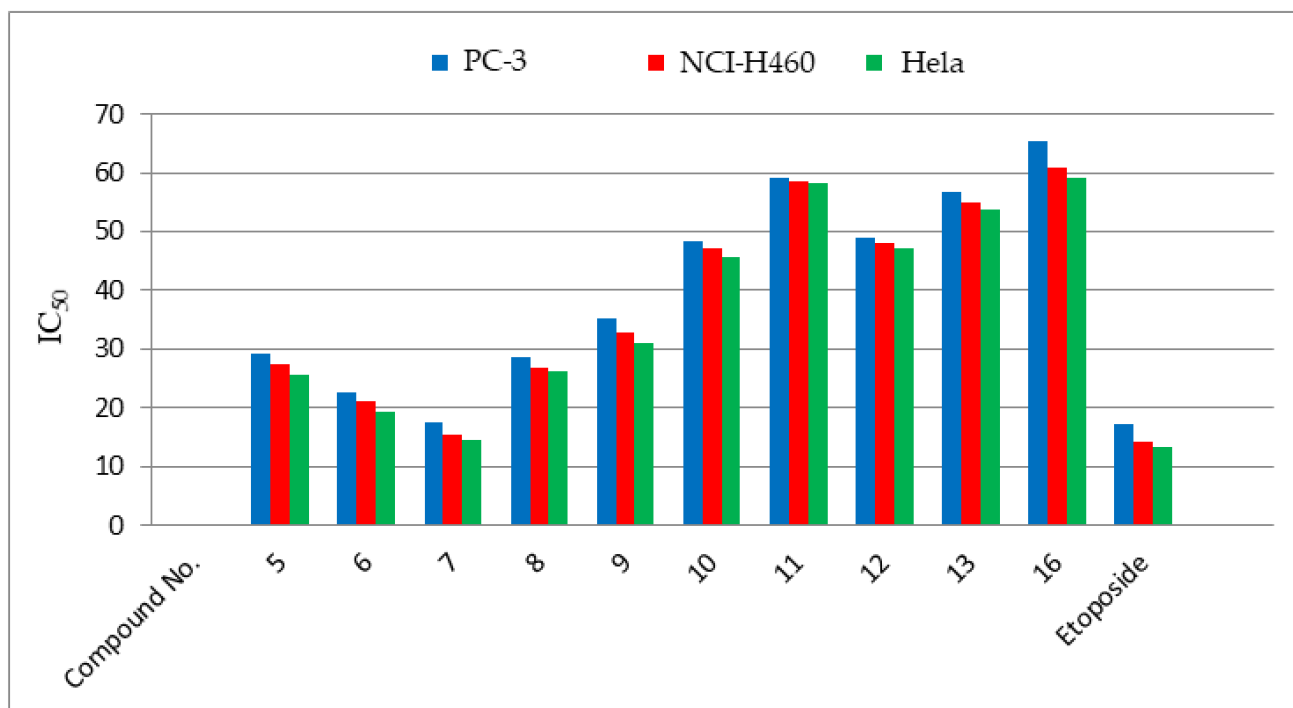


Figure 2. In vitro cytotoxic results of the target compounds **5–13**, **16** and etoposide towards PC-3, NCI-H460 and Hela cell lines.

Anticancer activity was calculated using the MTT assay. Results are the average of three independent experiments run in triplicate.

2.2.2. Structure–Activity Relationship

From the data obtained, it is clear that the naphthyridine derivatives **5–7** were the most active compounds against PC-3, NCI-H460 and Hela cell lines (IC_{50} = 17.5–29.31, 15.42–27.54 and 14.62–25.73, respectively). Within the naphthyridine derivatives, replacing the ethyl carboxylate moiety at C-3 as in compound **5** (IC_{50} = 25.73–29.31 μ M) with the nitrile as in compound **6** (IC_{50} = 19.31–22.73 μ M) and/or compound **7** (IC_{50} = 14.62–17.50 μ M) markedly enhanced the anticancer potential. On the other hand, the presence of an amino group at C-2 of the naphthyridine ring as in compound **6** (IC_{50} = 19.31–22.73 μ M) showed less potency than the 2-oxo moiety in compound **7** (IC_{50} = 14.62–17.50 μ M) against all tested cell lines. Moreover, replacing the naphthyridine ring with the pyrrolo[2,3-*b*]pyridine system decreased the anticancer activity. This is clear upon comparing compound **7** (IC_{50} = 14.62–17.50 μ M) with the pyrrolopyridine derivative **9** (IC_{50} = 31.05–35.12 μ M). Furthermore, replacing the cyano group at C-2 of the pyrrole ring as in compound **9** (IC_{50} = 31.05–35.12 μ M) with the carboxylate moiety as in compound **10** (IC_{50} = 45.62–48.29 μ M) decreased the cytotoxic potency. Moreover, fusing the pyrimidine derivative **11** (IC_{50} = 58.12–59.13 μ M) with the triazolo ring as in compound **16** (IC_{50} = 59.24–65.41 μ M) reduced the anticancer potential against all tested cell lines.

2.3. Molecular Docking Study

To determine the mechanism of action behind the anticancer activity of the novel constructed compounds, these candidates were docked within topoisomerase II with the use of MOE software, 2010, version 8. An X-ray crystal of topoisomerase II with the cocrystallized ligand etoposide was attained from Protein Data Bank (code: 3QX3). Justification of the docking process was performed by redocking etoposide within topoisomerase II with RMSD = 0.9526. Etoposide formed two hydrogen bonds with AspB479 and DG C13 with binding score = -16.69 kcal/mol (Table 2).

Table 2. Docking outcomes for compounds **5–13**, **16** and etoposide within topoisomerase II (code: 3QX3).

Target No.	E. Score Kcal/mol	Number of Hydrogen Bonds	Distance ($^{\circ}$) from Amino Acid	Bound Group
5	−16.16	2	1.88	DGC13
			1.75	ArgB503
6	−16.79	2	2.11	AspB479
			2.37	LysB456
7	−17.29	2	2.29	AspB479
			2.05	AspB479
8	−15.02	3	3.25	DCC11
			2.96	DCC11
			3.01	DGC10
9	−17.32	1	3.06	ArgB820
10	−14.06	2	2.84	ArgB503
			3.09	DGC13
11	−12.58	1	3.07	AlaB816
12	−14.22	2	1.98	ArgB820
			2.27	SerB818
13	−12.87	1	2.56	DGC13
16	−10.98	0	-	-
Etoposide	−16.69	2	1.89	AspB479
			1.87	DGC13

The outcomes from this study illustrate that the novel compounds **5–13** and **16** fitted well within topoisomerase II. The most potent anticancer compound **7** recorded the highest binding energy score (-17.29 kcal/mol), showing two H-bond interactions with AspB479

with the carbonyl and amino groups of the pyridine ring. Moreover, the thiazole moiety of compound 7 recorded arene cation binding with ArgB503 (Figure 3).

On the other hand, compound 6 performed two types of interactions with the topoisomerase II active site. One is hydrophobic binding of the thiophen moiety with DGC13, and the other binding involves hydrogen bond interactions as follows: (i) AspB479 with NH₂, and (ii) LysB456 with CN (Figure 4).

Moreover, compound 5 displayed hydrogen-bonding interactions with ArgB503 and DGC13 through binding with NH₂ and C=O groups. Moreover, this naphthyridine derivative recorded hydrophobic binding with a thiophen moiety with DAC12 with binding score = −16.16 kcal/mol (Figure 5).

Moreover, the pyrimidine derivative 8 recorded binding energy score = −15.02 kcal/mol, forming three hydrogen bonds as follows (Figure 6):

- (i) DCC11 with carbonyl group;
- (ii) DCC11 with amino group;
- (iii) DGC10 with cyano group.

On the other hand, the cyano group of compound 9 formed a hydrogen bond with ArgB820, with a binding score equal to −17.32 (Figure 7).

The pyrrole moiety of pyrrolopyridine derivative 10 performed arene cation binding with ArgA820 with binding score = −14.06 kcal/mol. In addition, it formed two H-bonds with ArgB503 and DGC13 (Figure 8).

Furthermore, the pyrrole derivative 12 formed two H-bonds with ArgB820 and SerB818 through the nitrogen atom of the pyrrole ring and the amino group with binding score = −14.22 kcal/mol (Figure 9).

Compound 11 recorded a hydrophobic interaction with DAC12 and one hydrogen bond with AlaB816 (Figure 10).

Moreover, the pyridine ring of candidate 13 showed a hydrophobic interaction with DAC12 in addition to forming only one H-bond with DGC13 (Figure 11).

Finally, the least potent cytotoxic agent 16 formed only a hydrophobic interaction between the thiophen ring and DAC12, without displaying any hydrogen bond (Figure 12).

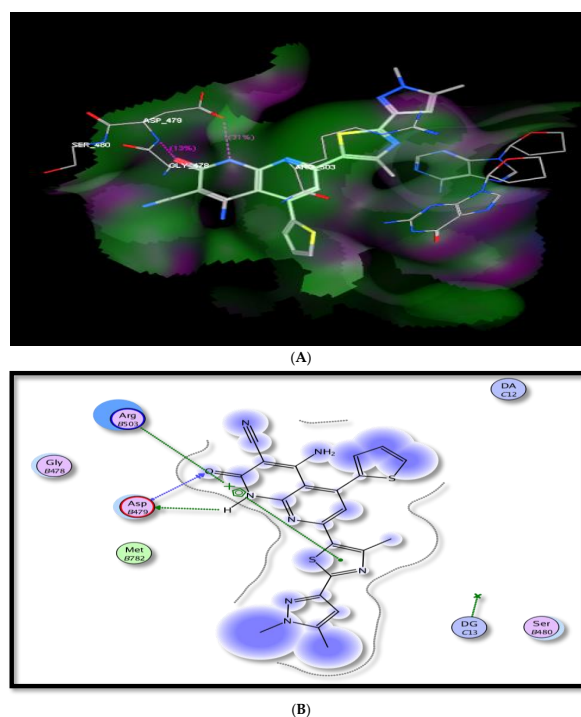


Figure 3. The suggested binding mode of compound 7 within topoisomerase II. (A) 3D binding mode within the active site. (B) 2D binding mode within topoisomerase II.

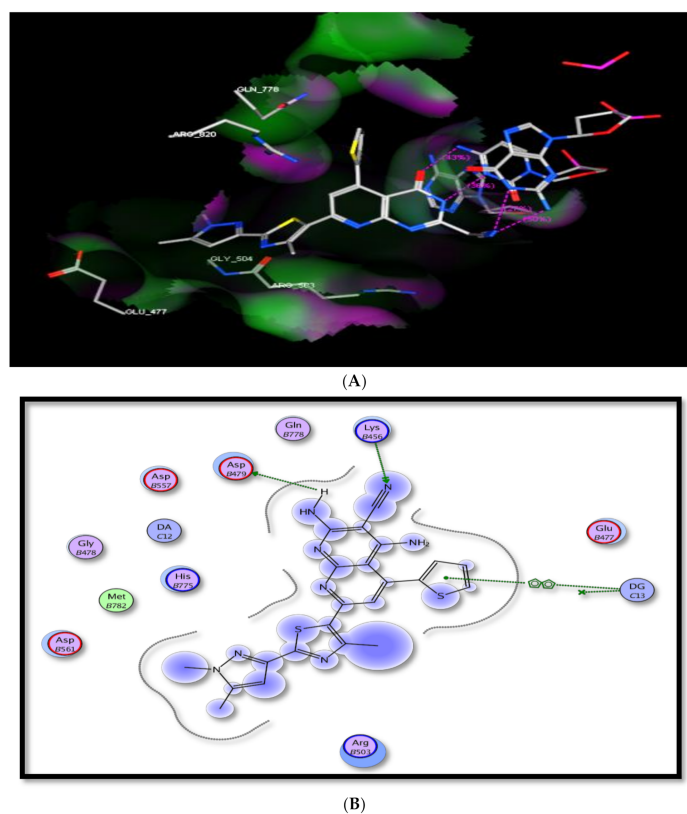


Figure 4. The suggested binding mode of compound 6 within topoisomerase II. (A) 3D binding mode within the active site. (B) 2D binding mode within topoisomerase II.

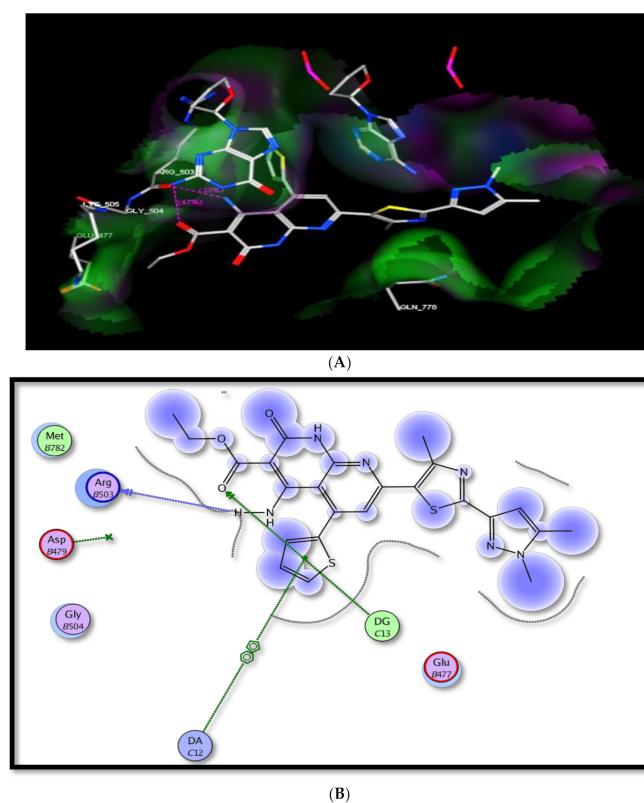


Figure 5. The suggested binding mode of compound 5 within topoisomerase II. (A) 3D binding mode within the active site. (B) 2D binding mode within Topoisomerase II.

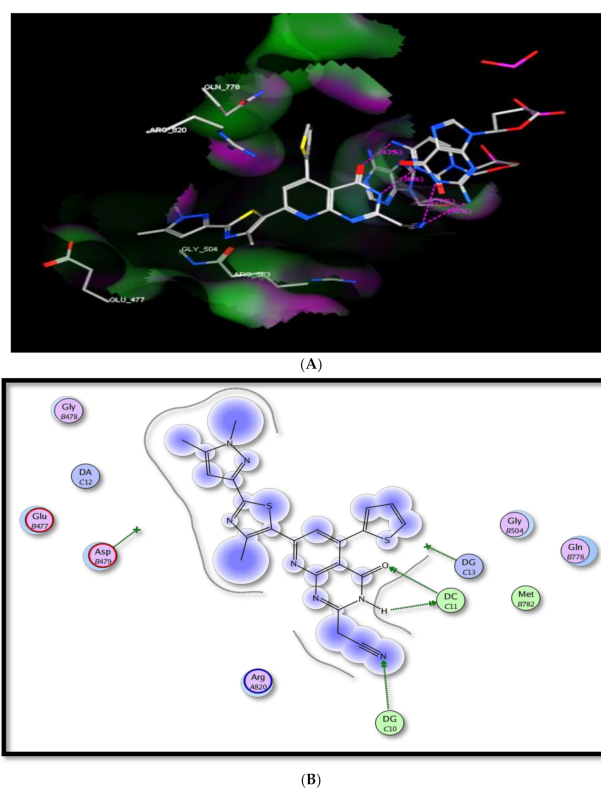


Figure 6. The suggested binding mode of compound **8** within topoisomerase II. **(A)** 3D binding mode within the active site. **(B)** 2D binding mode within topoisomerase II.

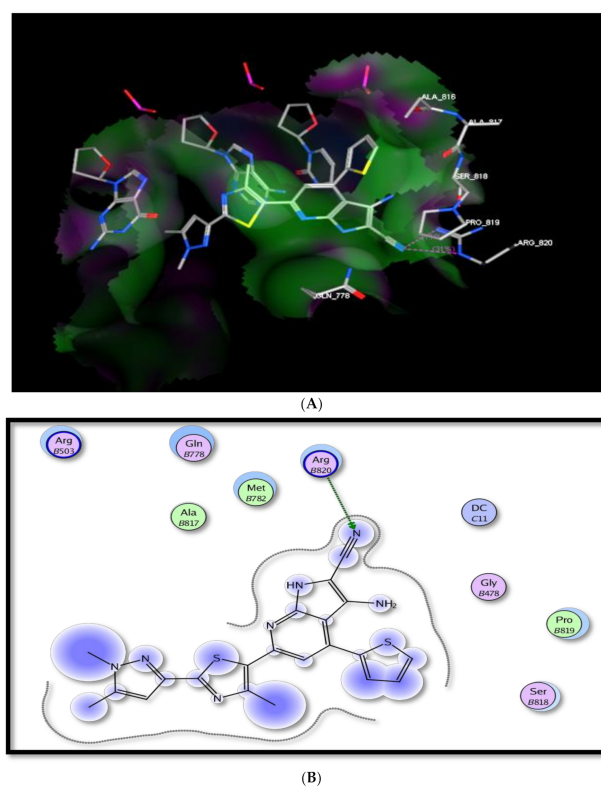


Figure 7. The suggested binding mode of compound **9** within topoisomerase II. **(A)** 3D binding mode within the active site. **(B)** 2D binding mode within topoisomerase II.

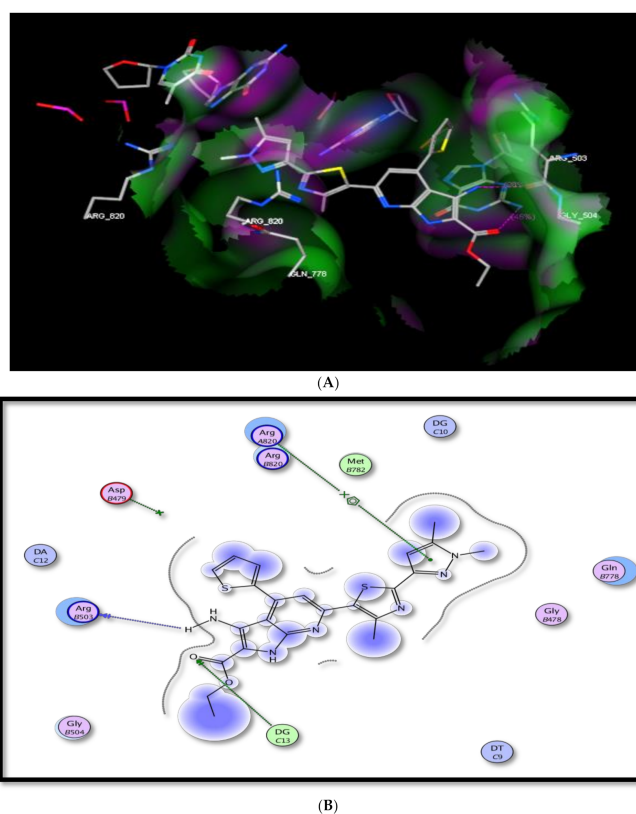


Figure 8. The suggested binding mode of compound 10 within topoisomerase II. **(A)** 3D binding mode within the active site. **(B)** 2D binding mode within topoisomerase II.

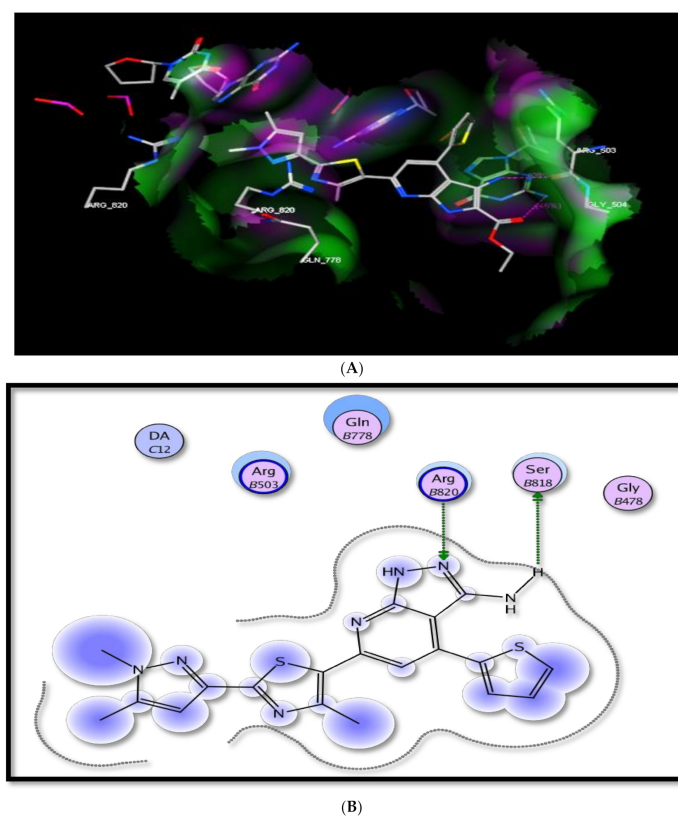


Figure 9. The suggested binding mode of compound 12 within topoisomerase II. **(A)** 3D binding mode within the active site. **(B)** 2D binding mode within topoisomerase II.

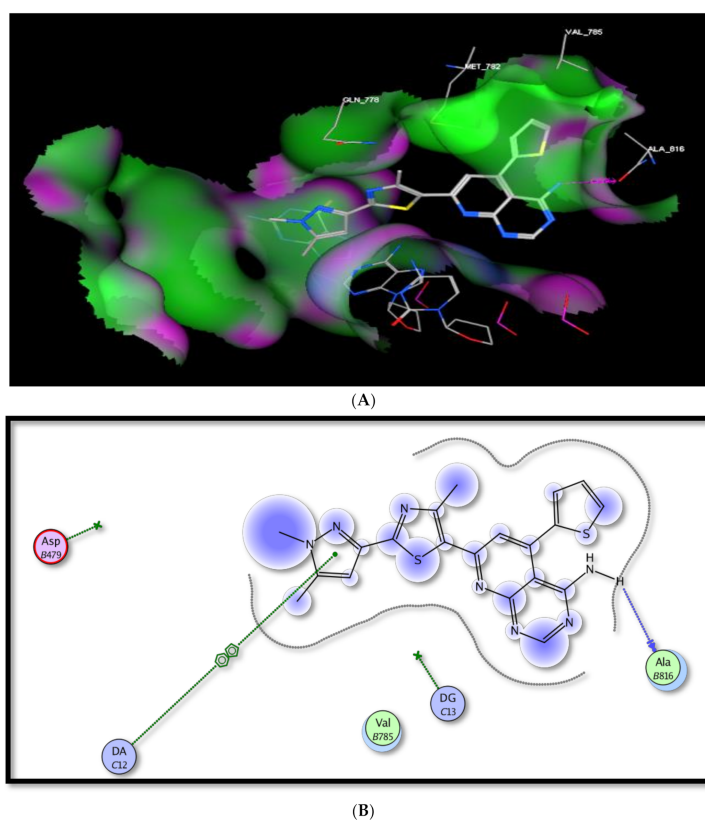


Figure 10. The suggested binding mode of compound 11 within topoisomerase II. (A) 3D binding mode within the active site. (B) 2D binding mode within topoisomerase II.

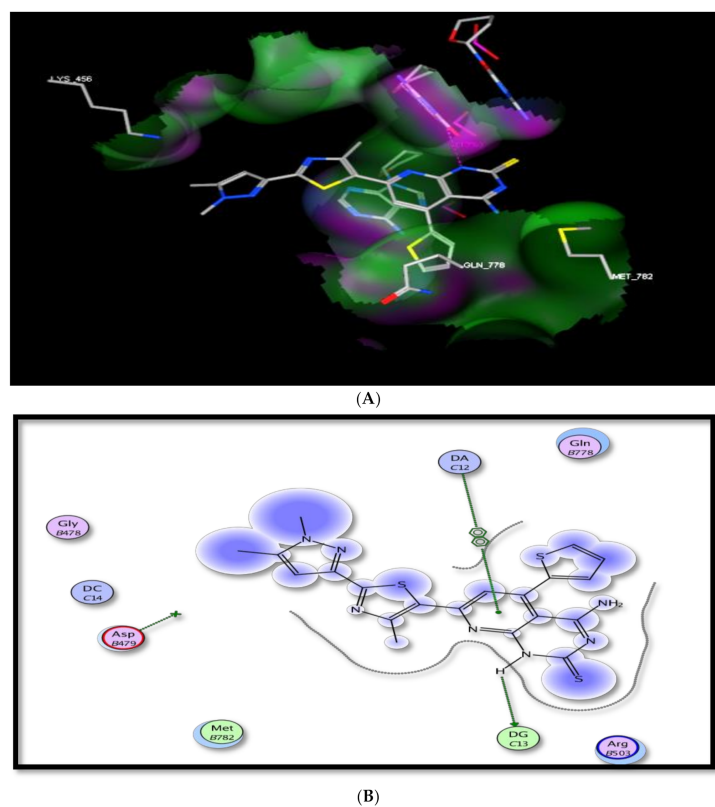


Figure 11. The suggested binding mode of compound 13 within topoisomerase II. (A) 3D binding mode within the active site. (B) 2D binding mode within topoisomerase II.

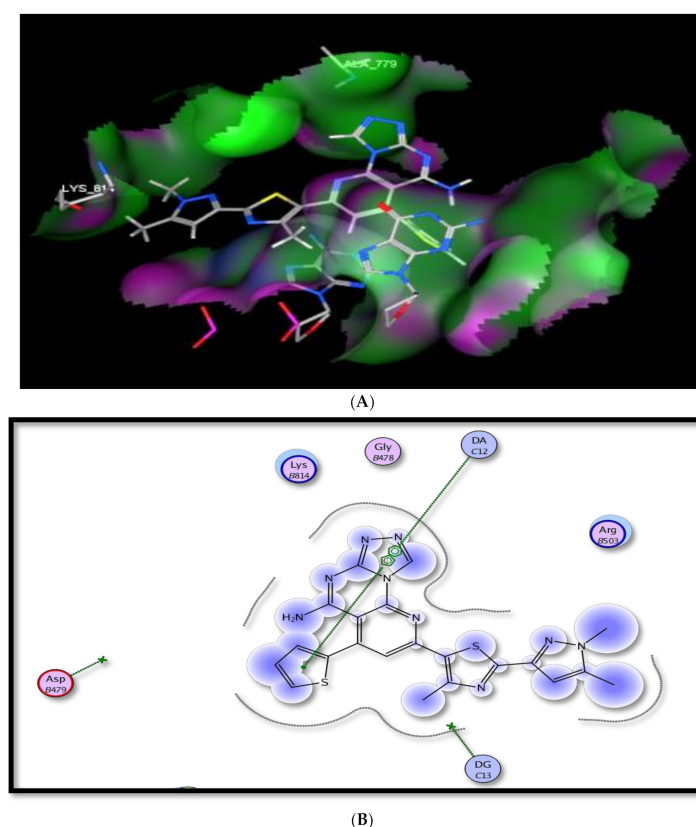


Figure 12. The suggested binding mode of compound **16** within topoisomerase II. (A) 3D binding mode within the active site. (B) 2D binding mode within topoisomerase II.

3. Materials and Methods

3.1. General Description of Materials and Methods

The chemicals used in this work were obtained from Sigma Aldrich (Palo Alto, CA, USA) and were used without any further purification.

3.2. Instrumentation

All the synthesized compounds were elucidated by NMR (^1H , ^{13}C), MS and IR (see supplementary materials). IR data were documented as KBr discs utilizing a Bruker-Vector 22 FTIR spectrophotometer (Bruker, Manassquan, NJ, USA). The NMR spectra were verified with a Varian Mercury VXR-300 (Bruker, Marietta, GA, USA), at 300 and 75 MHz (^1H and ^{13}C -NMR) spectra separately, as a solution in $\text{DMSO}-d_6$. The chemical shifts are presented in δ scale relative to the internal reference tetramethylsilane (TMS). Mass spectra were recorded at 70 eV on a Hewlett Packard MS-5988 spectrometer (Hewlett Packard, Palo Alto, CA, USA). Elemental analyses were conducted at the Micro-Analytical Center of Taif University, Taif, Saudi Arabia.

3.3. Synthetic Procedures and Analytic Data of Compounds

1-(2-(1,5-Dimethyl-1H-pyrazol-3-yl)-4-methylthiazol-5-yl)ethanone (2). In an ethanolic solution (40 mL), the pyrazole carbothiamide **1** (0.15 g, 1 mmol) and 3-chloro-2,4-pentanedione (1 mmol) were boiled at reflux for 7 h (tested by TLC). On cooling at ambient temperature, the obtained solid was filtered, washed with cold methanol and recrystallized using EtOH to furnish the acetyl thiazole analogy **2**, as a pale yellow solid. Yield: 75%; m.p. 242–244 °C; IR (KBr): (cm^{-1}) 683 (C–S–C), 1610–1625 (2C=N), 1730 (C=O); ^1H -NMR: δ 1.39, 2.02, 3.25 (s, 9H, 3Me), 3.12 (s, 3H, Ac), 6.62 (s, 1H, Pyraz. $_{(C_4)}$ -H); ^{13}C -NMR: 10.7, 15.8, 27.4, 38.3 (4Me), 106.8, 138.3, 143.4, 161.2 (2C=C), 136.3, 162.8 (2C=N), 196.5 (C=O); MS (m/z , %):

235.09 (M^+ , 15); Anal. Calcd. for $C_{11}H_{13}N_3OS$ (235.31): C, 56.15; H, 5.57; N, 17.86%. Found: C, 56.01; H, 5.32; N, 17.67%.

2-Amino-6-(2-(1,5-dimethyl-1H-pyrazol-3-yl)-4-methylthiazol-5-yl)-4-(thiophen-2-yl)-4H-pyran-3-carbonitrile (3). In a mixture of dry ethanol, piperidine (25 mL:0.5 mL), the acetyl thiazole **2** (0.23 g, 1 mmol), thiophene-2-carbaldehyde (0.12 g, 1 mmol) and malononitrile (0.06 g, 1 mmol) were mixed and refluxed for 3 h (examined by TLC). After cooling the reaction mixture to RT, it was transferred onto ice/ H_2O and neutralized by HCl, and the solid separated out was isolated, splashed with H_2O , dried out and recrystallized by EtOH to yield compound **3** as a buff powder. Yield: 77%; m.p. 172–174 °C; IR (KBr): (cm^{-1}) 675–681 (2C–S–C), 1610–1625 (2C=N), 2211 ($C\equiv N$), 3281 (NH_2); 1H -NMR: δ 2.42, 2.45, 3.64 (s, 9H, 3Me), 3.96 (d, 1H, $J = 8.5$, Pyran. $_{(C4)}$ -H), 5.01 (d, H, $J = 8.5$, Pyran. $_{(C5)}$ -H), 6.01 (s, 1H, Pyraz. $_{(C4)}$ -H), 6.51 (brs, 2H, NH_2 Deutr. Exch), 6.83–7.49 (m, 3H, Thioph.-H); ^{13}C -NMR: 10.7, 15.8, 38.3 (3Me), 29.8 (pyran C-4), 119.1 ($C\equiv N$), 58.1, 97.5, 106.3, 123.4, 125.5, 127.0, 138.2, 139.7, 143.0, 153.9, 159.2, 161.0 (6C=C), 136.3, 162.8 (2C=N); MS (m/z , %): 395.09 (M^+ , 20); Anal. Calcd. for $C_{19}H_{17}N_5OS_2$ (395.50): C, 57.70; H, 4.33; N, 17.71%. Found: C, 57.42; H, 4.15; N, 17.51%.

2-Amino-6-(2-(1,5-dimethyl-1H-pyrazol-3-yl)-4-methylthiazol-5-yl)-4-(thiophen-2-yl)nicotinonitrile (4). To a solution of the acetyl compound **2** (0.23 g, 1 mmol) in a mixture of dry EtOH (40 mL) containing $AcONH_4$ (0.53 g, 7 mmol), thiophene-2-carbaldehyde (0.12 g, 1 mmol) and malononitrile (0.06 g, 1 mmol) were added and mixed together. The reaction mixture was heated at reflux for 3 h (examined by TLC), then allowed to cool to RT, transferred onto mashed ice and neutralized by HCl, and the solid separated out was collected, splashed with H_2O , dried out and recrystallized using EtOH to yield compound **4** as a yellow powder. Yield: 81%; m.p. 158–160 °C; IR (KBr): (cm^{-1}) 675–681 (2C–S–C), 1610–1625 (2C=N), 2211 ($C\equiv N$), 3281 (NH_2); 1H -NMR: δ 2.26, 2.40, 2.46 (s, 9H, 3Me), 6.06 (s, 1H, Pyraz. $_{(C4)}$ -H), 6.49 (brs, 2H, NH_2 Deutr. Exch), 7.23–7.36 (m, 4H, Thioph.-H and Pyrid. $_{(C5)}$ -H); ^{13}C -NMR: 10.7, 13.8, 38.3 (3Me), 113.7 ($C\equiv N$), 86.3, 106.3, 111.7, 126.8, 127.2, 128.2, 128.6, 138.2, 138.5, 148.4, 153.3, 162.2 (6C=C), 136.3, 155.7, 162.8 (3C=N); MS (m/z , %): 392.09 (M^+ , 40); Anal. Calcd. for $C_{19}H_{16}N_6S_2$ (392.50): C, 58.14; H, 4.11; N, 21.41%. Found: C, 58.01; H, 4.02; N, 21.22%.

General method for the synthesis of compounds (5–7). To a solution of pyridine analogy **4** (0.39 g, 1 mmol), in a mixture of ethanol, piperidine (25 mL: 0.3 mL), some selected carbon donors—namely diethylmalonate, malononitrile and ethyl cyanoacetate—were added. Next, the reaction mixture was refluxed for 4–6 h (as tested by TLC), and the solvent was extracted under reduced pressure. The obtained solid was collected, dried and recrystallized by the proper solvent, providing the desired compounds (**5–7**).

Ethyl 4-amino-7-(2-(1,5-dimethyl-1H-pyrazol-3-yl)-4-methylthiazol-5-yl)-2-oxo-5-(thiophen-2-yl)-1,2-dihydro-1,8-naphthyridine-3-carboxylate (5). After recrystallization using AcOH, compound **5** was attained as yellow crystals. Yield: 79%; m.p. 216–218 °C; IR (KBr): (cm^{-1}) 675–681 (2C–S–C), 1610–1625 (3C=N), 1648 (amidic C=O), 1729 (ester C=O), 3320–3350 (NH and NH_2); 1H -NMR: δ 1.29 (t, 3H, $J = 6.5$, Me), 2.42, 2.45, 3.64 (s, 9H, 3Me), 3.06 (q, 2H, $J = 6.5$, CH_2), 6.01 (s, 1H, Pyraz. $_{(C4)}$ -H), 6.40 (brs, 2H, NH_2 Deutr. Exch), 6.83–7.49 (m, 4H, Thioph.-H and Pyrid. $_{(C5)}$ -H), 10.21 (brs, H, NH Deutr. Exch); ^{13}C -NMR: 10.8, 12.5, 14.2, 38.0 (4Me), 61.0 (CH_2), 86.2, 103.1, 106.3, 111.7, 127.6, 127.9, 128.0, 128.6, 138.2, 138.5, 148.6, 152.4, 162.0, 169.6 (7C=C), 136.3, 155.6, 162.8 (3C=N), 161.1, 165.0 (2C=O); MS (m/z , %): 506.12 (M^+ , 31); Anal. Calcd. for $C_{24}H_{22}N_6O_3S_2$ (506.60): C, 56.90; H, 4.38; N, 16.59%. Found: C, 56.61; H, 4.12; N, 16.29%.

2,4-Diamino-7-(2-(1,5-dimethyl-1H-pyrazol-3-yl)-4-methylthiazol-5-yl)-5-(thiophen-2-yl)-1,8-naphthyridine-3-carbonitrile (6). After recrystallization using ethanol–DMF (3:1), compound **6** was obtained as a yellow powder. Yield: 71%; m.p. 189–191 °C; IR (KBr): (cm^{-1}) 675–681 (2C–S–C), 1610–1625 (4C=N), 2210 ($C\equiv N$), 3320–3350 (2 NH_2); 1H -NMR: δ 2.26, 2.40, 2.46 (s, 9H, 3Me), 6.06 (s, 1H, Pyraz. $_{(C4)}$ -H), 5.35, 6.49 (brs, 4H, 2 NH_2 Deutr. Exch), 7.23–7.36 (m, 4H, Thioph.-H and Pyrid. $_{(C5)}$ -H); ^{13}C -NMR: 10.7, 13.8, 38.3 (3Me), 113.7 ($C\equiv N$), 77.8, 86.3, 106.8, 124.3, 126.8, 127.2, 128.2, 128.6, 138.2, 138.5, 148.4, 155.3, 158.3, 162.0 (7C=C), 136.3,

155.7, 162.2, 162.8 (4C=N); MS (m/z , %): 458.04 (M^+ , 47); Anal. Calcd. for $C_{22}H_{18}N_8S_2$ (458.56): C, 57.62; H, 3.96; N, 24.44%. Found: C, 57.41; H, 3.68; N, 24.30%.

4-Amino-7-(2-(1,5-dimethyl-1H-pyrazol-3-yl)-4-methylthiazol-5-yl)-2-oxo-5-(thiophen-2-yl)-1,2-dihydro-1,8-naphthyridine-3-carbonitrile (7). After recrystallization using DMF–MeOH (1:3), compound **7** was obtained as brownish-yellow fine grains. Yield: 73%; m.p. 159–161 °C; IR (KBr): (cm^{-1}) 675–681 (2C–S–C), 1610–1625 (3C=N), 2210 (C≡N), 3280 (NH₂); ¹H-NMR: δ 2.42, 2.45, 3.64 (s, 9H, 3Me), 5.62 (brs, 2H, NH₂ Deutr. Exch), 6.01 (s, 1H, Pyraz._(C4)-H), 6.83–7.49 (m, 4H, Thioph.-H and Pyrid._(C5)-H), 10.12 (brs, 1H, NH Deutr. Exch); ¹³C-NMR: 10.8, 12.5, 38.0 (3Me), 115.8 (C≡N), 80.7, 106.3, 111.1, 112.3, 127.6, 128.0, 128.6, 138.2, 138.4, 144.2, 149.8, 176.8 (6C=C), 136.3, 151.3, 162.8 (3C=N), 168.3 (C=O); MS (m/z , %): 459.10 (M^+ , 10); Anal. Calcd. for $C_{22}H_{17}N_7OS_2$ (459.55): C, 57.50; H, 3.73; N, 21.34%. Found: C, 57.29; H, 3.41; N, 21.15%.

2-(7-(2-(1,5-Dimethyl-1H-pyrazol-3-yl)-4-methylthiazol-5-yl)-4-oxo-5-(thiophen-2-yl)-3,4-dihydropyrido[2,3-d]pyrimidin-2-yl)acetonitrile (8). Without any solvent, the pyridine analogy **4** (0.39 g, 1 mmol) and ethyl cyanoacetate (10 mL) were fused for 5 h. After cooling to RT, the reaction mixture was triturated with cold ethanol, and the separated solid was extracted and recrystallized by EtOH, to provide the cyanomethyl pyrimidine analogy **8**, in an 82% yield; m.p. 253–256 °C; IR (KBr): (cm^{-1}) 675–681 (2C–S–C), 1610–1625 (4C=N), 1645 (C=O amide), 2210 (C≡N), 3280 (NH); ¹H-NMR: δ 2.42, 2.45, 3.64 (s, 9H, 3Me), 4.12 (s, 2H, CH₂), 6.01 (s, 1H, Pyraz._(C4)-H), 6.83–7.49 (m, 4H, Thioph.-H and Pyrid._(C5)-H), 10.12 (brs, 1H, NH Deutr. Exch); ¹³C-NMR: 10.8, 12.5, 38.0 (3Me), 22.4 (CH₂), 116.3 (C≡N), 106.3, 118.5, 121.5, 127.6, 127.9, 128.0, 128.6, 138.2, 138.4, 147.5, 152.4, 154.0 (6C=C), 136.3, 152.1, 156.4, 162.8 (4C=N), 161.0 (C=O); MS (m/z , %): 459.09 (M^+ , 41); Anal. Calcd. for $C_{22}H_{17}N_7OS_2$ (459.55): C, 57.50; H, 3.73; N, 21.34%. Found: C, 57.29; H, 3.41; N, 21.15%.

General Procedure for the Synthesis of Compounds (9 and 10). To a solution of compound **4** (0.39 g, 1 mmol) and anhydrous K₂CO₃ (1.37 g) in dry acetone (25 mL), chloroacetonitrile and/or ethyl bromoacetate (20 mmol) was added. After, the reaction mixture was refluxed for 5 h (monitored by TLC), and the extra solvent was removed under reduced pressure. The resulted rough matter was triturated by cold MeOH, and the separated solid was filtered, washed, dried and recrystallized to give compounds **9** and **10**.

3-Amino-6-(2-(1,5-dimethyl-1H-pyrazol-3-yl)-4-methylthiazol-5-yl)-4-(thiophen-2-yl)-1H-pyrrolo[2,3-b]pyridine-2-carbonitrile (9). After recrystallization using methanol compound **9** obtained as an off-white solid. Yield: 78%; m.p. 261–263 °C; IR (KBr): (cm^{-1}) 675–681 (2C–S–C), 1612–1625 (3C=N), 2208 (C≡N), 3320–3350 (NH and NH₂); ¹H-NMR: 2.26, 2.40, 2.46 (s, 9H, 3Me), 6.06 (s, 1H, Pyraz._(C4)-H), 6.61 (brs, 2H, NH₂ Deutr. Exch), 7.23–7.36 (m, 4H, Thioph.-H and Pyrid._(C5)-H), 9.61 (brs, 1H, NH Deutr. Exch); ¹³C-NMR: 10.7, 13.8, 38.3 (3Me), 113.7 (C≡N), 101.8, 106.8, 118.6, 124.3, 126.8, 127.2, 128.2, 128.6, 138.2, 138.6, 148.4, 153.3, 158.3, 162.9 (7C=C), 136.3, 155.7, 162.2, 162.8 (4C=N); MS (m/z , %): 431.11 (M^+ , 41); Anal. Calcd. for $C_{21}H_{17}N_7S_2$ (431.54): C, 58.45; H, 3.97; N, 22.72%. Found: C, 58.21; H, 3.69; N, 22.42%.

Ethyl 3-amino-6-(2-(1,5-dimethyl-1H-pyrazol-3-yl)-4-methylthiazol-5-yl)-4-(thiophen-2-yl)-1H-pyrrolo[2,3-b]pyridine-2-carboxylate (10). After recrystallization using dioxane, compound **11** was obtained as a pale yellow solid. Yield: 73%; m.p. 275–257 °C; IR (KBr): (cm^{-1}) 675–681 (2C–S–C), 1612–1625 (3C=N), 1664 (C=O), 3320–3341 (NH and NH₂); ¹H-NMR: δ 1.29 (t, 3H, J = 6.5, Me), 2.42, 2.45, 3.64 (s, 9H, 3Me), 4.32 (q, 2H, J = 6.5, CH₂), 6.01 (s, 1H, Pyraz._(C4)-H), 6.32 (brs, 2H, NH₂ Deutr. Exch), 6.83–7.49 (m, 4H, Thioph.-H and Pyrid._(C5)-H), 10.62 (brs, 1H, NH Deutr. Exch); ¹³C-NMR: 10.8, 12.5, 14.1, 38.0 (4Me), 60.9 (CH₂), 106.3, 108.3, 118.5, 121.5, 130.2, 127.6, 127.9, 128.0, 128.6, 138.2, 138.4, 147.5, 152.4, 154.0 (7C=C), 136.3, 151.1, 162.8 (C=N), 161.0 (C=O); MS (m/z , %): 478.12 (M^+ , 32); Anal. Calcd. for $C_{23}H_{22}N_6O_2S_2$ (478.59): C, 57.72; H, 4.63; N, 17.56%. Found: C, 57.43; H, 4.51; N, 17.33%.

7-(2-(1,5-Dimethyl-1H-pyrazol-3-yl)-4-methylthiazol-5-yl)-5-(thiophen-2-yl)pyridol[2,3-d]pyrimidin-4-amine (11). The pyridine analogue **4** (0.39 g, 1 mmol) and formamide (10 mL) were fused face to face for 3 h. Afterwards, the separated brown solid on cooling was collected and dried. A brown solid with an 80% yield was obtained after recrystallization using EtOH; m.p. over 300 °C; IR (KBr): (cm^{-1}) 675–681 (2C–S–C), 1610–1625 (5C=N), 3385 (NH₂); ¹H-

NMR: δ 2.42, 2.45, 3.64 (s, 9H, 3Me), 6.01 (s, 1H, Pyraz._(C4)-H), 6.32 (brs, 2H, NH₂ Deutr. Exch), 6.83–7.49 (m, 5H, Thioph.-H, Pyrid._(C5)-H and Pyrimi._(C2)-H); ¹³C-NMR: 10.8, 12.5, 38.0 (3Me), 105.2, 106.3, 121.5, 127.7, 127.9, 128.0, 128.6, 138.2, 141.9, 144.9, 152.4, 157.8 (6C=C), 136.3, 151.2, 152.3, 157.4, 162.8 (5C=N); MS (*m/z*, %): 419.10 (M⁺, 9); Anal. Calcd. for C₂₀H₁₇N₇S₂ (419.53): C, 57.26; H, 4.08; N, 23.37%. Found: C, 57.11; H, 4.02; N, 23.17%.

6-(2-(1,5-Dimethyl-1H-pyrazol-3-yl)-4-methylthiazol-5-yl)-4-(thiophen-2-yl)-1H-pyrazolo[3,4-b]pyridin-3-amine (12). Compound **4** (0.39 g, 1 mmol) was refluxed for 3h with NH₂OH.HCl (0.07 g, 0.1 mmol) in AcOH acid (25 mL) having anhydrous AcONa (0.08 g, 0.1 mmol) as a catalyst. Afterwards, the reaction mixture was decanted onto cold H₂O, and the formed precipitate was filtered, dried and recrystallized from EtOH, affording a reddish-brown powder in a 91% yield; m.p. 286–288 °C; IR (KBr): (cm⁻¹) 675–681 (2C–S–C), 1610–1625 (4C=N), 3320–3355 (NH and NH₂); ¹H-NMR: δ 2.42, 2.45, 3.64 (s, 9H, 3Me), 6.01 (s, 1H, Pyraz._(C4)-H), 6.41 (brs, 2H, NH₂ Deutr. Exch), 6.83–7.49 (m, 4H, Thioph.-H and Pyrid._(C5)-H), 12.61 (brs, H, NH Deutr. Exch); MS (*m/z*, %): 407.10 (M⁺, 53); Anal. Calcd. for C₁₉H₁₇N₇S₂ (407.52): C, 56.00; H, 4.20; N, 24.06%. Found: C, 55.82; H, 4.11; N, 23.79%.

General Method for the Synthesis of Compounds (13–16). To a solution of the pyridine derivative **4** (0.39 g, 1 mmol), in AcOH acid (25 mL), equimolar amounts of some amino nucleophiles—namely urea, 6-methylpyridin-2-amine, 3-phenyl-1H-pyrazol-5-amine, and/or 1,2,4-triazin-3-amine—were added. Afterwards, the reaction mixture was refluxed for 6–8 h (Monitored by TLC analysis). After the solvent was evaporated in vacuo, the rough product was mashed with cold MeOH. The formed solid was isolated and then recrystallized to obtain compounds (13–16).

4-Amino-7-(2-(1,5-dimethyl-1H-pyrazol-3-yl)-4-methylthiazol-5-yl)-5-(thiophen-2-yl)pyrido[2,3-d]pyrimidine-2(1H)-thione (13). This was obtained as an orange-yellow solid after recrystallization using ethanol in a 72% yield; m.p. 197–199 °C; IR (KBr): (cm⁻¹) 675–681 (2C–S–C), 1345 (thioamidic C=S), 1612–1625 (4C=N), 3210–3348 (NH, NH₂); ¹H-NMR: 2.26, 2.40, 2.46 (s, 9H, 3Me), 6.06 (s, 1H, Pyraz._(C4)-H), 6.61 (brs, 2H, NH₂ Deutr. Exch), 7.23–7.59 (m, 4H, Thioph.-H and Pyrid._(C5)-H), 10.27 (brs, 1H, NH Deutr. Exch); ¹³C-NMR: 10.7, 13.8, 38.3 (3Me), 106.8, 118.6, 124.3, 127.2, 128.2, 128.6, 138.2, 138.6, 148.4, 153.3, 158.3, 162.9 (6C=C), 136.3, 155.7, 162.2, 162.8 (4C=N), 180.4 (C=S); MS (*m/z*, %): 451.07 (M⁺, 23); Anal. Calcd. for C₂₀H₁₇N₇S₃ (451.59): C, 53.19; H, 3.79; N, 21.71%. Found: C, 53.10; H, 3.51; N, 21.48%.

2-(2-(1,5-Dimethyl-1H-pyrazol-3-yl)-4-methylthiazol-5-yl)-10-methyl-4-(thiophen-2-yl)-5H-dipyrido[1,2-a:3',2'-e]pyrimidin-5-imine (14). This was obtained as a yellow powder after recrystallization using dioxane in a 65% yield; m.p. 263–265 °C; IR (KBr): (cm⁻¹) 675–6810 (2C–S–C), 1612–1625 (5C=N), 3219 (NH); ¹H-NMR: δ 2.26, 2.42, 2.45, 3.64 (s, 12H, 4Me), 6.01 (s, 1H, Pyraz._(C4)-H), 6.83–7.49 (m, 7H, Thioph.-H and Pyrid._(C3-5)-H), 8.92 (brs, H, N=H Deutr. Exch); MS (*m/z*, %): 483.13 (M⁺, 41); Anal. Calcd. for C₂₅H₂₁N₇S₃ (483.61): C, 62.09; H, 4.38; N, 20.27%. Found: C, 61.79; H, 4.11; N, 20.10%.

8-(2-(1,5-Dimethyl-1H-pyrazol-3-yl)-4-methylthiazol-5-yl)-2-phenyl-6-(thiophen-2-yl)pyrazolo[1,5-a]pyrido[3,2-e]pyrimidin-5-amine (15). This was obtained as a yellow solid after recrystallization using MeOH/dioxane (3:1) in an 80% yield; m.p. 215–217 °C; IR (KBr): (cm⁻¹) 675–681 (2C–S–C), 1610–1625 (5C=N), 3385 (NH₂); ¹H-NMR: δ 2.42, 2.45, 3.64 (s, 9H, 3Me), 6.01 (s, 1H, Pyraz._(C4)-H), 6.52 (brs, 2H, NH₂ Deutr. Exch), 6.83–7.49 (m, 11H, Ar-H, Thioph.-H, Pyrid._(C5)-H and Pyrimi._(C2)-H); ¹³C-NMR: 10.8, 12.5, 38.0 (3Me), 92.5, 105.2, 106.3, 121.7, 127.5, 127.6, 127.9, 128.0, 128.6, 128.7, 129.2, 133.0, 138.2, 141.9, 144.9, 149.4, 152.4, 159.2 (10C=C), 136.3, 152.3, 155.6, 157.4, 162.8 (5C=N); MS (*m/z*, %): 534.14 (M⁺, 17); Anal. Calcd. for C₂₈H₂₂N₈S₂ (534.66): C, 62.90; H, 4.15; N, 20.96%. Found: C, 62.71; H, 4.02; N, 20.69%.

2-(2-(1,5-Dimethyl-1H-pyrazol-3-yl)-4-methylthiazol-5-yl)-4-(thiophen-2-yl)pyrido[3,2-e][1,2,4]triazolo[4,3-a]pyrimidin-5-amine (16). This was obtained as faint yellow crystals after recrystallization using EtOH in a 75% yield; m.p. 218–220 °C; IR (KBr): (cm⁻¹) 675–681 (2C–S–C), 1610–1625 (6C=N), 3385 (NH₂); 2.26, 2.40, 2.46 (s, 9H, 3Me), 6.06 (s, 1H, Pyraz._(C4)-H), 6.61 (brs, 2H, NH₂ Deutr. Exch), 7.27–7.59 (m, 5H, Thioph.-H, Pyrid._(C5)-H and Triaz._(C3)-H); ¹³C-NMR: 10.7, 13.8, 38.3 (3Me), 106.8, 118.6, 124.3, 127.2, 128.2, 128.6, 138.2, 138.6, 148.4, 153.3, 158.3, 162.9 (6C=C), 136.0, 136.3, 155.3, 157.0, 162.2, 162.8 (6C=N); MS (*m/z*, %): 459.12

(M⁺, 55); Anal. Calcd. for C₂₁H₁₇N₉S₂ (459.55): C, 54.89; H, 3.73; N, 27.43%. Found: C, 54.59; H, 3.41; N, 27.22%.

3.4. Assessment of Anticancer Activity

MTT Cytotoxicity Assay

The *in vitro* growth inhibitory activity of the ten achieved analogues was explored in comparison with a notable anti-malignancy standard medication, etoposide, adapting the colorimetric MTT assay in triplicate as described previously [48]. In brief, cells were seeded onto 96-well tissue culture plates in DMEM containing 10% FBS to a final volume of 0.2 mL. The cells were subjected to different treatments after 24 h of seeding. The cells were then incubated for 48 h with etoposide (positive controls), test drugs or vehicle (DMSO). The media were then removed, replaced with 200 μ L DMEM containing 0.5 mg/mL of MTT and cells were incubated for 2 h. Next, the supernatants were removed and the precipitated formazan was dissolved by adding 200 μ L of DMSO. Absorbance at 570 nm was determined using a microplate reader (Model 450 Microplate Reader; Bio-Rad). Results were calculated by subtracting blank readings.

3.5. Docking Study

Topoisomerase II crystal structure with the cocrystallized ligand (etoposide) was downloaded from Protein Data Bank (PDB code: 3QX3). The target derivatives **5–13** and **16** were docked within the topoisomerase II active site using the MOE 2010 program. To validate the docking step, etoposide was redocked with RMSD = 0.9526. Three-dimensional structures of the target derivatives were built, protonated and energy minimized and saved as mdb files to be docked within topoisomerase II. The results of the docking study are given in Table 2.

3.6. Statistical Analysis

The presented results are mean \pm SD, and the statistical analysis was performed using one-way ANOVA followed by Dunnett's multiple comparisons test. Differences were considered significant at $p < 0.05$. Statistical analysis was performed using SPSS for Windows (SPSS, Inc., Chicago, IL, USA).

4. Conclusions

In this work, we described an efficient and facile approach for the synthesis of 2-amino-6-(2-(1,5-dimethyl-1*H*-pyrazol-3-yl)-4-methylthiazol-5-yl)-4-(thiophen-2-yl)nicotinonitrile (**4**), via one-pot multicomponent condensation, as a reactive precursor to synthesize novel pyrazolothiazole-based pyridine conjugates (**5–16**). All the target derivatives **5–13** and **16** were evaluated for their cytotoxic activity towards prostate cancer (PC-3), lung cancer (NCI-H460) and cervical cancer (Hela) cell lines. All the tested compounds revealed anticancer activity towards PC-3 (IC₅₀ = 17.50–65.41 μ M), NCI-H460 (IC₅₀ = 15.42–61.05 μ M) and Hela (IC₅₀ = 14.62–59.24 μ M). Analysis of the structure–activity relationship (SAR) indicated that the naphthyridine hybrids had more favorable cytotoxic potential than pyridopyrimidine, pyrrolopyridine and/or pyrido[3,2-*e*][1,2,4]triazolo[4,3-*a*] pyrimidine hybrids. A docking study was performed within the topoisomerase II active site to predict the binding mechanism of these compounds. All the docked compounds demonstrated good fitting within topoisomerase II. The most potent cytotoxic compound **7** (IC₅₀ = 14.62–17.50 μ M) displayed the best docking score (−17.29 Kcal/mol), forming two hydrogen bonds with the AspB479 amino acid, while the least potent cytotoxic compound **16** (59.24–65.41 μ M) did not show any hydrogen bond with the enzyme and bound with DAC12 via hydrophobic binding with the lowest binding score (−10.98 Kcal/mol).

Supplementary Materials: The following are available online. MS, ¹H NMR, ¹³C NMR of compounds **2**, **4**, **6**, **9**, **13**, **16**.

Author Contributions: Conceptualization: I.H.E.A.; preparation and characterization of the heterocyclic compounds: I.H.E.A. and N.A.A.E.; writing—original draft, design of the experiments, formal analysis and discussion of the results: I.H.E.A., N.A.A.E. and R.B.B.; contributions to the antitumor study and completing of the docking study: R.B.B. All authors have read and agreed to the published version of the manuscript.

Funding: This research was funded by Taif University grant number TURSP-2020/27.

Institutional Review Board Statement: Not applicable.

Informed Consent Statement: Not applicable.

Data Availability Statement: The data presented in this study are available in this article.

Acknowledgments: This work was supported by Taif University researchers supporting project number (TURSP-2020/27), Taif University, Taif, Saudi Arabia.

Conflicts of Interest: The authors declare no conflict of interest.

Sample Availability: Samples of the compounds are not available from authors.

References

1. Wang, T.T.; Liu, J.; Zhong, H.Y.; Chen, H.; Lv, Z.L.; Zhang, Y.K.; Zhang, M.F.; Geng, D.P.; Niu, C.J.; Li, Y.M.; et al. Synthesis and anti-tumor activity of novel ethyl 3-aryl-4-oxo-3,3a,4,6-tetrahydro-1H-furo[3,4-c]pyran-3a-carboxylates. *Bioorg. Med. Chem. Lett.* **2011**, *21*, 3381. [[CrossRef](#)] [[PubMed](#)]
2. Sangthong, S.; Krusong, K.; Ngamrojanavanich, N.; Vilaivan, T.; Puthong, S.; Chandchawan, S.; Muangsin, N. Synthesis of rotenoid derivatives with cytotoxic and topoisomerase II inhibitory activities. *Bioorg. Med. Chem. Lett.* **2011**, *21*, 4813. [[CrossRef](#)]
3. Li, X.; He, L.; Chen, H.; Wu, W.; Jiang, H. Copper-catalyzed aerobic C(sp²)-H functionalization for C-N bond formation: Synthesis of pyrazoles and indazoles. *J. Org. Chem.* **2013**, *78*, 3636–3646. [[CrossRef](#)] [[PubMed](#)]
4. Santos, C.M.M.; Freitas, M.; Fernandes, E. A comprehensive review on xanthone derivatives as α -glucosidase inhibitors. *Eur. J. Med. Chem.* **2018**, *157*, 1460–1479. [[CrossRef](#)] [[PubMed](#)]
5. Kalaria, P.N.; Karad, S.C.; Raval, D.K. A review on diverse heterocyclic compounds as the privileged scaffolds in antimalarial drug discovery. *Eur. J. Med. Chem.* **2018**, *158*, 917–936. [[CrossRef](#)] [[PubMed](#)]
6. Kerru, N.; Bhaskaruni, S.V.H.S.; Gummidi, L.; Maddila, S.N.; Maddila, S.; Jonnalagadda, S.B. Recent advances in heterogeneous catalysts for the synthesis of imidazole derivatives. *Synth. Commun.* **2019**, *49*, 2437–2459. [[CrossRef](#)]
7. Kerru, N.; Singh, P.; Koorbanally, N.; Raj, R.; Kumar, V. Recent advances (2015–2016) in anticancer hybrids. *Eur. J. Med. Chem.* **2017**, *142*, 179–212. [[CrossRef](#)]
8. Ma, Y.Z.; Tang, Z.B.; Sang, C.Y.; Qi, Z.Y.; Hui, L.; Chen, S.W. Synthesis and biological evaluation of nitroxide labeled pyrimidines as Aurora kinase inhibitors. *Bioorg. Med. Chem. Lett.* **2019**, *29*, 694–699. [[CrossRef](#)]
9. Kerru, N.; Maddila, S.; Jonnalagadda, S.B. Design of carbon-carbon and carbon-heteroatom bond formation reactions under green conditions. *Curr. Org. Chem.* **2019**, *23*, 3156–3192. [[CrossRef](#)]
10. Xu, Z.; Zhao, S.J.; Liu, Y. 1,2,3-Triazole-containing hybrids as potential anticancer agents: Current developments, action mechanisms and structure-activity relationships. *Eur. J. Med. Chem.* **2019**, *183*, 111700. [[CrossRef](#)]
11. Zarate, D.Z.; Aguilar, R.; Hernandez-Benitez, R.I.; Labarrios, E.M.; Delgado, F.; Tamariz, J. Synthesis of α -ketols by functionalization of captodative alkenes and divergent preparation of heterocycles and natural products. *Tetrahedron* **2015**, *71*, 6961–6978. [[CrossRef](#)]
12. Abdellatif, K.R.A.; Fadaly, W.A.; Kamel, G.M.; Elshaiar, Y.A.; El-Magd, M.A. Design, synthesis, modeling studies and biological evaluation of thiazolidine derivatives containing pyrazole core as potential anti-diabetic PPAR- γ agonists and anti-inflammatory COX-2 selective inhibitors. *Bioorg. Chem.* **2019**, *82*, 86–99. [[CrossRef](#)]
13. Fang, W.Y.; Ravindar, L.; Rakesh, K.P.; Manukumar, H.M.; Shantharam, C.S.; Alharbi, N.S.; Qin, H.L. Synthetic approaches and pharmaceutical applications of chloro-containing molecules for drug discovery: A critical review. *Eur. J. Med. Chem.* **2019**, *173*, 117–153. [[CrossRef](#)]
14. Kerru, N.; Singh-Pillay, A.; Awolade, P.; Singh, P. Current anti-diabetic agents and their molecular targets: A review. *Eur. J. Med. Chem.* **2018**, *152*, 436–488. [[CrossRef](#)]
15. Takate, S.J.; Shinde, A.D.; Karale, B.K.; Akolkar, H.; Nawale, L.; Sarkar, D.; Mhaske, P.C. Thiazolyl-pyrazole derivatives as potential antimycobacterial agents. *Bioorg. Med. Chem. Lett.* **2019**, *29*, 1199–1202. [[CrossRef](#)]
16. Nagaraju, K.; Lalitha, G.; Suresh, M.; Kranthi, K.G.; Sreekantha, B.J. A Review on Recent Advances in Nitrogen-Containing Molecules and Their Biological Applications. *Molecules* **2020**, *25*, 1909. [[CrossRef](#)]
17. Shu, L.; Chen, C.; Huan, X.; Huang, H.; Wang, M.; Zhang, J.; Yan, Y.; Liu, J.; Zhang, T.; Zhang, D. Design, synthesis, and pharmacological evaluation of 4- or 6-phenylpyrimidine derivatives as novel and selective Janus kinase 3 inhibitors. *Eur. J. Med. Chem.* **2020**, *191*, 112148. [[CrossRef](#)]

18. Wang, R.; Yu, S.; Zhao, X.; Chen, Y.; Yang, B.; Wu, T.; Hao, C.; Zhao, D.; Cheng, M. Design, synthesis, biological evaluation and molecular docking study of novel thieno[3,2-d]pyrimidine derivatives as potent FAK inhibitors. *Eur. J. Med. Chem.* **2020**, *188*, 112024. [[CrossRef](#)]
19. Diao, P.C.; Lin, W.Y.; Jian, X.E.; Li, Y.H.; You, W.W.; Zhao, P.L. Discovery of novel pyrimidine-based benzothiazole derivatives as potent cyclin-dependent kinase 2 inhibitors with anticancer activity. *Eur. J. Med. Chem.* **2019**, *179*, 196–207. [[CrossRef](#)]
20. Kaur, R.; Chaudhary, S.; Kumar, K.; Gupta, M.K.; Rawal, R.K. Recent synthetic and medicinal perspectives of dihydropyrimidines: A review. *Eur. J. Med. Chem.* **2017**, *132*, 108–134. [[CrossRef](#)]
21. Chaudhari, K.; Surana, S.; Jain, P.; Patel, H.M. Mycobacterium tuberculosis (MTB) GyrB inhibitors: An attractive approach for developing novel drugs against TB. *Eur. J. Med. Chem.* **2016**, *124*, 160–185. [[CrossRef](#)] [[PubMed](#)]
22. Sameem, B.; Saeedi, M.; Mahdavi, M.; Shafiee, A. A review on tacrine-based scaffolds as multi-target drugs (MTDLs) for Alzheimer's disease. *Eur. J. Med. Chem.* **2017**, *128*, 332–345. [[CrossRef](#)] [[PubMed](#)]
23. Akhtar, J.; Khan, A.A.; Ali, Z.; Haider, R.; Yar, M.S. Structure-activity relationship (SAR) study and design strategies of nitrogen-containing heterocyclic moieties for their anticancer activities. *Eur. J. Med. Chem.* **2017**, *125*, 143–189. [[CrossRef](#)] [[PubMed](#)]
24. Ma, X.; Lv, X.; Zhang, J. Exploiting polypharmacology for improving therapeutic outcome of kinase inhibitors (KIs): An update of recent medicinal chemistry efforts. *Eur. J. Med. Chem.* **2018**, *143*, 449–463. [[CrossRef](#)] [[PubMed](#)]
25. Kaur, R.; Dahiya, L.; Kumar, M. Fructose-1,6-bisphosphatase inhibitors: A new valid approach for management of type 2 diabetes mellitus. *Eur. J. Med. Chem.* **2017**, *141*, 473–505. [[CrossRef](#)] [[PubMed](#)]
26. Modi, P.; Patel, S.; Chhabria, M. Structure-based design, synthesis and biological evaluation of a newer series of pyrazolo[1,5-a]pyrimidine analogues as potential anti-tubercular agents. *Bioorg. Chem.* **2019**, *87*, 240–251. [[CrossRef](#)] [[PubMed](#)]
27. Yang, F.; Yu, L.Z.; Diao, P.C.; Jian, X.E.; Zhou, M.F.; Jiang, C.S.; You, W.W.; Wei-Feng, M.; Zhao, P.L. Novel[1,2,4]triazolo[1,5-a]pyrimidine derivatives as potent antitubulin agents: Design, multicomponent synthesis and antiproliferative activities. *Bioorg. Chem.* **2019**, *92*, 103260. [[CrossRef](#)] [[PubMed](#)]
28. Hananya, N.; Shabat, D. A Glowing Trajectory between Bio- and Chemiluminescence: From LuciferinBased Probes to Triggerable Dioxetanes. *Angew. Chem. Int. Ed.* **2017**, *56*, 16454–16463. [[CrossRef](#)]
29. Chen, K.; Yao, X.; Tang, T.; Chen, L.-M.; Xiao, C.; Wang, J.-Y.; Chen, H.-F.; Jiang, Z.-X.; Liu, Y.; Zheng, X. Thiazole-based and thiazolidine-based protein tyrosine phosphatase 1B inhibitors as potential antidiabetes agents. *Med. Chem. Res.* **2020**, 1–16. [[CrossRef](#)]
30. Sayed, A.R.; Gomha, S.M.; Taher, E.A.; Muhammad, Z.A.; El-Seedi, H.R.; Gaber, H.M.; Ahmed, M.M. One-Pot Synthesis of Novel Thiazoles as Potential Anticancer Agents. *Drug Des. Dev. Ther.* **2020**, *14*, 1363–1375. [[CrossRef](#)]
31. Lino, C.I.; Gonçalves de Souza, I.; Borelli, B.M.; Silvério Matos, T.T.; Santos Teixeira, I.N.; Ramos, J.P.; Maria de Souza Fagundes, E.; de Oliveira Fernandes, P.; Maltarollo, V.G.; Johann, S.; et al. Synthesis, molecular modeling studies and evaluation of antifungal activity of a novel series of thiazole derivatives. *Eur. J. Med. Chem.* **2018**, *151*, 248–260. [[CrossRef](#)]
32. Maghraby, M.T.E.; Abou-Ghadir, O.M.F.; Abdel-Moty, S.G.; Ali, A.Y.; Salem, O.I.A. Novel class of benzimidazole-thiazole hybrids: The privileged scaffolds of potent anti-inflammatory activity with dual inhibition of cyclooxygenase and 15-lipoxygenase enzymes. *Bioorg. Med. Chem.* **2020**, *28*. [[CrossRef](#)]
33. Dhameliya, T.M.; Tiwari, R.; Banerjee, A.; Pancholia, S.; Sriram, D.; Panda, D.; Chakraborti, A.K. Benzo[d]thiazole-2-carbanilides as new anti-TB chemotypes: Design, synthesis, biological evaluation, and structure-activity relationship. *Eur. J. Med. Chem.* **2018**, *155*, 364–380. [[CrossRef](#)]
34. Grozav, A.; Porumb, I.-D.; Gäină, L.I.; Filip, L.; Hanganu, D. Cytotoxicity and Antioxidant Potential of Novel 2-(2-((1H-indol-5yl)methylene)-hydrazinyl)-thiazole Derivatives. *Molecules* **2017**, *22*, 260. [[CrossRef](#)]
35. Guerrero-Pepinosa, N.Y.; Cardona-Trujillo, M.C.; Garzon-Castano, S.C.; Veloza, L.A.; Sepúlveda-Arias, J.C. Antiproliferative activity of thiazole and oxazole derivatives: A systematic review of in vitro and in vivo studies. *Biomed. Pharmacother.* **2021**, *138*, 111495. [[CrossRef](#)]
36. Luzina, E.L.; Popov, A.V. Synthesis and anticancer activity of N-bis(trifluoromethyl)alkyl-N'-thiazolyl and N-bis(trifluoromethyl)alkyl-N'-benzothiazolyl ureas. *Eur. J. Med. Chem.* **2009**, *44*, 4944–4953. [[CrossRef](#)]
37. Satoh, A.; Nagatomi, Y.; Hirata, Y.; Ito, S.; Suzuki, G.; Kimura, T.; Maehara, S.; Hikichi, H.; Satow, A.; Hata, M.; et al. Discovery and in vitro and in vivo profiles of 4-fluoro-N-[4-[6-(isopropylamino)pyrimidin-4-yl]-1,3-thiazol-2-yl]-N-methylbenzamide as novel class of an orally active metabotropic glutamate receptor 1 (mGluR1) antagonist. *Bioorg. Med. Chem. Lett.* **2009**, *19*, 5464–5468. [[CrossRef](#)]
38. Havrylyuk, D.; Zimenkovsky, B.; Vasylenko, O.; Zaprutko, L.; Gzella, A.; Lesyk, R. Synthesis of novel thiazolone-based compounds containing pyrazoline moiety and evaluation of their anticancer activity. *Eur. J. Med. Chem.* **2009**, *44*, 1396–1404. [[CrossRef](#)]
39. George, R.F.; Samir, E.M.; Abdelhamed, M.N.; Abdel-Aziz, H.A.; Abbas, S.E.-S. Synthesis and anti-proliferative activity of some new quinoline based 4,5-dihydropyrazoles and their thiazole hybrids as EGFR inhibitors. *Bioorg. Chem.* **2019**, *83*, 186–197. [[CrossRef](#)]
40. Kaminsky, D.; Zimenkovsky, B.; Lesyk, R. Synthesis and in vitro anticancer activity of 2,4-azolidinedione-acetic acids derivatives. *Eur. J. Med. Chem.* **2009**, *44*, 3627–3636. [[CrossRef](#)]
41. El Azab, I.H.; Elkanzi, N.A.A. Design, Synthesis, and Antimicrobial Evaluation of New Annulated Pyrimido[2,1-c][1,2,4]triazolo[3,4-f][1,2,4]triazines. *Molecules* **2020**, *25*, 1339. [[CrossRef](#)] [[PubMed](#)]

42. El Azab, I.H.; Elkanzi, N.A.A. An Efficient Synthetic Approach Towards Benzo[b]pyrano[2,3-e][1,4]diazepines and Their Cytotoxic Activity. *Molecules* **2020**, *25*, 2051. [[CrossRef](#)] [[PubMed](#)]
43. El Azab, I.H.; Elkanzi, N.A.A.; Gobouri, A.A. Design and Synthesis of Some New Quinoxaline-Based Heterocycles. *J. Heterocycl. Chem.* **2018**, *55*, 65–76. [[CrossRef](#)]
44. El Azab, I.H.; Gobouri, A.A.; Altalhi, T.A. 4-Chlorothiazole-5-carbaldehydes as Potent Precursors for Synthesis of Some New Pendant N-heterocycles Endowed with Anti-Tumor Activity. *J. Heterocycl. Chem.* **2019**, *56*, 281–295. [[CrossRef](#)]
45. El Azab, I.H.; Elkanzi, N.A.A.; Gobouri, A.A.; Altalhi, T.A. Convenient Synthesis of Novel Nitrogen Bridgehead Heterocycles Utilizing 3-Mercapto-6H-[1,2,4,5]oxatriazino[3,2-a]isoindol-6-one as a New Synthon. *J. Heterocycl. Chem.* **2019**, *56*, 60–72. [[CrossRef](#)]
46. El Azab, I.H.; Abu Ali, O.A.; El-Zahrani, A.H.; Gobouri, A.A.; Altalhi, T.A. Pyrazole-1-carbothioamide as a Potent Precursor for Synthesis of Some New N-heterocycles of Potential Biological Activity. *J. Heterocycl. Chem.* **2019**, *56*, 18–31. [[CrossRef](#)]
47. El Azab, I.H.; Khalifa, M.E.; Gobouri, A.A.; Altalhi, T.A. Synthesis, Characterization, and Pharmacological Evaluation of Some New Pteridine-Based Heterocycles as Antimicrobial Agents. *J. Heterocycl. Chem.* **2019**, *56*, 1352–1361. [[CrossRef](#)]
48. Mohamed, A.A.; Rania, B.B.; Olla, A.A.; Wafaa, R.M. Design, synthesis and antitumor activity of novel pyrazolo[3,4-d]pyrimidine derivatives as EGFR-TK inhibitors. *Bioorg. Chem.* **2016**, *66*, 88–96. [[CrossRef](#)]
49. Omar, H.A.; Arafa, E.-S.A.; Salama, S.A.; Arab, H.H.; Wu, C.-H.; Weng, J.-R. OSU-A9 inhibits angiogenesis in human umbilical vein endothelial cells via disrupting Akt–NF- κ B and MAPK signaling pathways. *Toxicol. Appl. Pharmacol.* **2013**, *272*, 616–624. [[CrossRef](#)]